Aerosol and Air Quality Research, 16: 2855–2868, 2016

ISSN: 1680-8584 print / 2071-1409 online
doi: 10.4209/aaqr.2015.06.0406

Aerosol Climatology over the Bay of Bengal and Arabian Sea Inferred from Space-Borne Radiometers and Lidar Observations

Shani Tiwari[1], Amit K. Mishra[2], Abhay K. Singh[1*]

[1] *Atmospheric Research Lab., Department of Physics, Banaras Hindu University, Varanasi-221005, India*
[2] *Department of Earth and Planetary Sciences, Weizmann Institute of Science, Rehovot 76100, Israel*

ABSTRACT

Atmospheric aerosols over the oceanic region are very important air pollutant and play a vital role in Earth's radiation budget and climate change. This study presents the aerosol climatology over the Bay of Bengal (BoB) and Arabian sea (AS) using long term (2006–2012) data from space-borne radiometers [Moderate-Resolution Imaging Spectroradiometer (MODIS), Ozone Monitoring Instrument (OMI)] and space-based active lidar onboard Cloud-Aerosol Lidar and Infrared Pathfinder Satellite Observation (CALIPSO). AS experiences higher AOD as compared to that over BoB during the study period. A good periodicity along with strong intra-seasonal/annual variability in aerosol loading is also observed over both the study regions. Approximately one month lag is found for maximum aerosol loading period over AS and BoB for almost every year i.e., June–July for AS and May–June for BoB. This lag could be explained by pathway and timing of summer monsoon over the Indian subcontinent. Elevated layers of absorbing dust up to 2–4 km altitudes are observed during the pre-monsoon and monsoon seasons over both the regions. The CALIPSO measurements show strong seasonal heterogeneity in aerosol properties over both the regions, which is well corroborated with MODIS and OMI observations. This significant seasonal heterogeneity in aerosol loading has been explained by the role of transportation of aerosols from various emission sources using NOAA HYSPLIT back trajectory model at three different altitude levels viz. 500, 1500 and 2500 m height. The possible role of Indian summer monsoon in modulating the aerosol behaviour over AS and BoB is another important aspect of this study that need further analyses using higher spatio-temporal resolution data.

Keywords: MODIS; CALIPSO; AOD; Aerosol Index (AI); Fine Mode Fraction (FMF).

INTRODUCTION

Atmospheric aerosols have a significant role in global and regional climate changes which are closely related to their optical and micro-physical properties through various atmospheric interactions (Moorthy *et al.*, 2009; Wild *et al.*, 2009; Kaskaoutis *et al.*, 2011 and reference therein). Aerosols show spatial and temporal variability which are highly associated with their different emission sources e.g. natural and anthropogenic (Ramanathan *et al.*, 2001; Kaskaoutis *et al.*, 2011; Tiwari *et al.*, 2015; 2013 and references therein). The climatic effects of aerosols are closely related to their optical properties and composition (Koch and Del Genio, 2010). The accurate quantification of the impact of aerosols on climate is one of the challenging issues in the twenty-first century due to the complex non-linear interaction between atmospheric parameters responsible of aerosol-climate interaction (Boucher *et al.*, 2013). Due to limited *in situ* aerosol observation and high aerosol loading, it is essential to improve the aerosol characterisation over the Indian subcontinent. The systematic ground-based measurements of aerosol properties in India started after development of a multi-wavelength radiometer by the Indian Space Research Organization (ISRO) which was deployed successfully at Trivandrum to measure spectral aerosol optical depth (AOD) (Moorthy *et al.*, 1999). The Indian Ocean Experiment (Ramanathan *et al.*, 2001) first addressed the issue of climatic effects of aerosols in this region in a comprehensive manner, which led to enhanced, coordinated efforts for *in-situ* multi-instrument and multiplatform measurements by ISRO under the Geosphere Biosphere Program (GBP) (Moorthy *et al.*, 2005). ISRO has conducted several focused campaigns in recent years over India and its surrounding oceans to characterize the chemical, microphysical and optical properties of aerosols. Many ship-based campaigns have been conducted in the Arabian Sea (Satheesh *et al.*, 2006; Babu *et al.*, 2008 and references therein) and in the Bay of Bengal (Satheesh *et al.*, 2006; Nair *et al.*, 2008; Kaskaoutis *et al.*, 2011 and references therein) for different seasons. Dey *et al.* (2004) analyzed the Ocean Color Monitor data onboard

* Corresponding author.
Tel.: +91-0542-2368390
E-mail address: abhay_s@rediffmail.com

Indian Remote Sensing Satellite Polar Series 4 (IRS-P4) to retrieve the aerosol parameters over the Arabian Sea (AS) and the Bay of Bengal (BoB).

Aerosol loading over AS shows a strong seasonal variation which is highly influenced by dust storms, coming mainly from the Middle East and southwest Asia during pre-monsoon and monsoon seasons (Babu *et al.*, 2008; Dey and di Girolamo, 2010; Kaskaoutis *et al.*, 2011; Prijith *et al.*, 2013; Kaskaoutis *et al.*, 2014 and reference therein). However, during post-monsoon and winter season it is influenced by Asian outflow (mainly from anthropogenic sources) by long range transportation. Recently, Prijith *et al.* (2013) reported that AS experienced largest aerosol loading in the month of July (> 0.8) due to the transport from the western Asian desert region. Similar results are also reported by Nair *et al.* (2005) over AS. The physico-chemical properties of aerosols at any location highly depend on their sources and extremely influenced by regional meteorology. A large heterogeneity in their three-dimensional distribution is very common due to their variable sources, emission characteristic, atmospheric lifetime and various atmospheric processes (Smirnov *et al.*, 2009). The AS is also influenced by the anthropogenic activities along with the densely inhabited regions in the west coast of India, West Asia, and East Africa, each having distinctly different living habits and energy-use patterns (Babu *et al.*, 2008). Several cruise experiments were carried out over surrounding Indian Oceanic regions in recent times to understand aerosol spatial and temporal distribution (Ramanathan *et al.*, 1995; 2001; Satheesh *et al.*, 2001; Vinoj *et al.*, 2004; Kedia and Ramachandran, 2008). Bay of Bengal (BoB) experiences a unique weather pattern associated with strong seasonal wind pattern. Nair *et al.* (2013) reported the results of extensive measurements of aerosol number size distributions over the oceanic regions of the BoB and AS during two large cruise experiments (one during pre-monsoon and the other during winter) to investigate the spatial distribution of aerosol size distributions. The size distributions over BoB showed a bimodal structure with prominent mode (100–125 nm) in the accumulation regime and weak mode (30–40 nm) in the Aitken regime during both pre-monsoon and winter seasons. In contrast to the BoB, a prominent Aitken mode was seen over the AS, where mineral dust intrudes quite frequently. First-time inter-comparison of Moderate-Resolution Imaging Spectroradiometer (MODIS) derived AODs with those measured from the surface over BoB were reported by Vinoj *et al.* (2004). Recently, Kaskaoutis *et al.* (2011) also reported that BoB experienced high aerosol loading with a highly spatial and temporal variability in their optical characteristic coming mainly from anthropogenic emission and their dispersion process controlled by meteorology. The understanding of aerosol spatial and temporal variability no doubt increased in last few years but not up to a satisfactory level mainly over BoB and AS. Therefore, there is a need to study the aerosol distributions along with their emission sources especially over the oceanic regions near the coastlines of India using longer time series.

In the present study, we focus on understanding long term (2006–2012) aerosol characteristics over AS and BoB and their seasonal variability along with vertical distribution using satellite observations from the MODIS, Cloud-Aerosol Lidar and Infrared Pathfinder Satellite Observation (CALIPSO), and Ozone Monitoring Instrument (OMI). We have also analyzed seasonal synoptic weather patterns over both the regions, which highly influence aerosol loading and their size distribution. For the better understanding of aerosol sources, their types and transport pathways, seven days air mass back-trajectories are also analyzed using HYSPLIT model.

INSTRUMENTATION AND METHODOLOGY

MODerate Resolution Imaging Spectroradiometer

In the present study, Aerosol Optical Depth (AOD) is obtained from MODIS level 3 data on board of both Aqua and Terra satellite and measures radiance at 36 spectral bands in the visible to thermal IR spectral range of 0.41–14 μm (Kaufman *et al.*, 1997). MODIS has a swath of 2330 km which make it possible to observe global data in a single day and passes over the Indian region at ~10:30 am (Terra) and ~01:30 pm (Aqua) local solar time. Inversion of MODIS data provides aerosol parameters at seven wavelength bands over oceanic regions and at three bands over land. As the spectral surface reflectance over land is highly heterogeneous, separate algorithms are used for the retrieval of aerosol parameters from MODIS data over ocean and land (Remer *et al.*, 2005). Owing to the relatively stable and homogeneous reflectance of the ocean surface, the accuracy of AOD derived from the MODIS data over the ocean is better than that over land (Prijith *et al.*, 2013). The MODIS-derived quality assured Level-3 (1° × 1°) gridded daily clear sky mean AOD (at 0.55 μm) and fine mode fraction (FMF) from Collection 051 provided by NASA are used here. Details about instrumentations, algorithms and error estimations are described by Kaufman and Tanre (1998), and updates are discussed by Remer *et al.* (2005).

Cloud-Aerosol Lidar and Infrared Pathfinder Satellite Observation (CALIPSO)

The vertical profiles of aerosol distribution are very important for the quantification of aerosol types and their radiative effects. CALIPSO is used to obtain the vertical distribution of aerosol over various regions of the Indian subcontinent (Mishra and Shibata, 2012a, b; Prijith *et al.*, 2013). It is the first lidar [Cloud-Aerosol Lidar with Orthogonal Polarization (CALIOP)] satellite to measure aerosol and cloud properties. CALIPSO's orbit has a 16-day repeat cycle, which produces sub-satellite tracks spaced longitudinally by 172 km at the equator. However, as CALIPSO observations are limited to the sub-satellite track, its spatial coverage is very poor compared to MODIS. CALIPSO can not provide observations at altitude regions that are below optically thick clouds. CALIOP level 2 Ver. 3.01 data product (Young and Vaughan, 2008) from 2006–2012 are used to present aerosol vertical distribution climatology over AS and BoB. Only night-time aerosol backscatter at 532 nm is used in this study to avoid possible noise in day-time data. All night-time aerosol backscatter profiles are screened for

the artifacts using the methodology provided by Mishra *et al.* (2014). More details about the CALIPSO algorithm and it's description are described by Winker *et al.* (2006) and Labonne *et al.* (2007).

Ozone Monitoring Instrument (OMI)

The Ozone Monitoring Instrument (OMI) aboard Aura is a nadir viewing, wide swath 20 hyperspectral imaging spectrometer that provides daily global coverage with high spectral resolutions and spatial resolution of 13 km × 24 km at nadir (Levelt *et al.*, 2006). OMI takes advantage of the greater sensitivity of radiances measured at the troposphere in the near UV region to the varying load and type of aerosols to derive Extinction Aerosol Optical Depth (EAOD), Single Scattering Albedo (SSA) and Absorbing Aerosol Optical Depth (AAOD) using an inversion procedure at 354, 388 and 500 nm generated by the near UV (OMAERUV) algorithm (Torres *et al.*, 2007). The OMAERUV retrieval algorithm is particularly sensitive to carbonaceous and mineral aerosols, and the aerosol layer height. The OMAERUV retrieval algorithm assumes that the column aerosol load can be represented by one of three types of aerosols and uses a set of aerosol models to account for the presence of these aerosols: carbonaceous aerosol from biomass burning, desert dust, and light absorbing sulphate-based aerosols. For carbonaceous and desert dust particles, the aerosol load is assumed to be vertically distributed following a Gaussian function characterized by peak (aerosol layer height) and half-width (aerosol layer geometric thickness) values (Torres *et al.*, 2013). In the present study, we have used level 3 OMI UV Aerosol Index (AI) product from 2006–2012 over AS and BoB.

Meteorological Data and Hysplit Backtrajectories Model

To understand the effect of synoptic meteorological conditions on aerosol distribution over the study region, National Center for Environmental Prediction (NCEP)/ National Centre of Atmospheric Research (NCAR) reanalysis daily mean data of wind vector and geopotential height at 850 hPa are used from January 2006 to December 2012.

We have used the daily seven days air mass back trajectories for 2006 to 2012 at three different altitudes 500 m, 1500 m, and 2500 m based on National Oceanic and Atmospheric Administration (NOAA) Hybrid Single Particle Lagrangian Integrated Trajectories (HYSPLIT) model (website http://ready.arl.noaa.gov/HYSPLIT.php) using NCEP reanalysis wind as input (Draxler and Rolph, 2003). It provides a three-dimensional (latitude, longitude and altitude) information of the pathways of air mass as a function of time. The transported aerosols and their distribution at the different altitudes over the study region is shown and discussed in the following section.

RESULTS AND DISCUSSION

Synoptic Pattern Seasonality

Synoptic meteorological conditions are very important for the study of aerosol characterization for any location. The wind synoptic meteorological conditions are very crucial parameters for the study of aerosol characterization and play a very critical role on the monsoon features over Indian region as well as global through radiation budget (Moorthy and Satheesh, 2000). Seasonally changing wind pattern has enough potential to carry a variety of the aerosols from different mainlands to oceans (Sreekanth *et al.*, 2013). This is due to the changes in air mass types, the impact of advection and transport, and the proximity to continental areas (Smirnov *et al.*, 1995, Satheesh *et al.*, 2006). Fig. 1 shows the mean composite of synoptic wind pattern and geopotential height at 850 hPa over the Indian subcontinent and nearby regions during the pre-monsoon (PrM: MAM), monsoon (M: JJA), post-monsoon (PoM: SON) and winter (W: DJF) season for 2006–2012. The region of interest (ROI) over AS and BoB are shown by red rectangles in respective plots. Fig. 1 reflects that AS experienced northerly and north-westerly wind in the PrM season. In the monsoon season, winds are generally south-westerly over AS following the onset pattern of Indian summer monsoon and reached over BoB through entering into the Indian subcontinent. During the PoM season, winds are mainly northerly and north-easterly over AS, which got dominated by strong northerly and north-easterly wind in the winter season. Winds are south-westerly during PrM, M and PoM over the BoB, which experience north-westerly wind during the winter season.

Climatology of Aerosol Optical Depth (AOD)

Fig. 2 represents the time series analyses of monthly mean variation of AOD at 550 nm associated with standard deviation from MODIS on board of both aqua and terra satellites over the study regions. AODs show a very good periodicity in variability over both the regions and have maximum value in the month of June over BoB, however over AS maximum loading is observed in July. Earlier studies reported that AS and BoB have highest mean seasonal aerosol loading during June–August with a large contribution of dust aerosol coming from Middle East, Arabia and southwest Asia (Tindale and Pease, 1999; Dey and di Girolamo, 2010; Satheesh *et al.*, 2010; Kaskaoutis *et al.*, 2011; Prijith *et al.*, 2013). AOD observations over both study regions show a very good seasonal and interannual variability with an increasing trend during 2006–2012 (Fig. 2). The annual mean variation of AOD along with their standard deviation is given in Table 1 for both the regions. Annual mean highest aerosol loading is found maximum in 2009 (0.39 ± 0.10) followed by 2008 (0.37 ± 0.16) over BoB. However, AS experiences highest aerosol loading in 2008 (0.48 ± 0.36) followed by 2011 (0.48 ± 0.29). The monthly mean variation of AOD over both the regions for 2006–2012 is given in Fig. 3 and details are summarised in Table 2. Fig. 3(a) shows that there is an increase in AOD loading from January to June and then it decreases slowly until November–December over BoB. BoB experiences maximum aerosol loading in June (0.54 ± 0.13) which may be due to long-range dust transportation (Fig. 1) and the growth of aerosol particles due to condensation/coagulation process (Dey and Girolamo, 2010). After that it decreases and reaches a minimum value in November (0.25 ± 0.03) over BoB and again it slightly

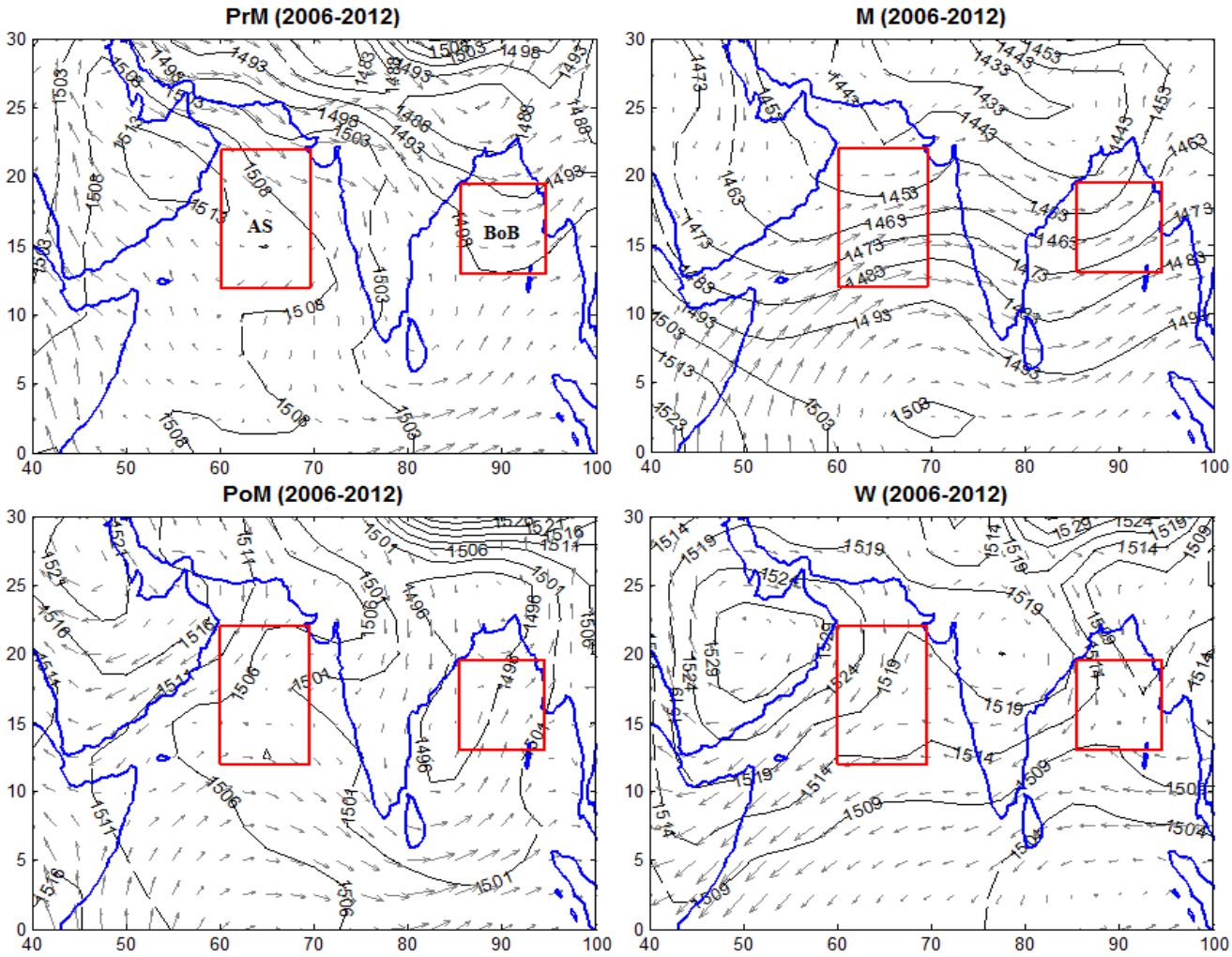

Fig. 1. Mean composite of synoptic wind pattern and geopotential height at 850 hPa over the Indian subcontinent and nearby regions during the pre-monsoon (PrM), monsoon (M), post monsoon (PoM) and winter (W) season for 2006–2012. Contours present geopotential height and wind vectors are shown by arrows. The region of interest (ROI) over Arabian Sea (AS) and Bay of Bengal (BoB) is shown by red rectangles in respective plots.

increases in December. A similar pattern is also observed over AS (Fig. 3(b)), which experiences maximum aerosol loading in the month of July (0.94 ± 0.07) followed by June (0.76 ± 0.29). However, AOD decreases after July and reaches the minimum in December (0.25 ± 0.02) over AS. Relatively smaller AOD values are observed over both the regions in winter which may be due to calm meteorological conditions that inhibit the long range transportation of aerosol from settlement areas. This result could be rationalised by the wind vector plots shown in Fig. 1. Prijith *et al.* (2013) also reported maximum aerosol loading in July over AS with annual peak > 0.8. The lag of one month for maximum aerosol loading between AS and BoB could be understood as synoptic summer monsoon system (Fig. 1, upper right panel) first reached over AS around the first week of June and then reached over BoB around last of June or starting of July. In general, summer monsoon wind system is accompanied by heavy rain and could be a significant source of wet removal of aerosol particles from the atmosphere. Results show abnormally higher AOD over AS during 2008 especially in June and July. We observe that in June 2008; mean AOD is 1.35, which is nearly 78% greater than the corresponding long-term mean value in June. Similarly, Prijith *et al.* (2013) reported highest AOD value in June 2008 with a regional mean AOD of 1.1, which was 97% larger than that of the corresponding long-term mean value in June from March 2000 to February 2011. A slightly smaller value was observed by Prijith *et al.* (2013) due to the selection of different region of interest over AS. Recently, Kaskaoutis *et al.* (2014) reported abnormal high aerosol loading over AS in June 2008 which is highly influenced by the specific role of the atmospheric dynamics and Sistan dust storms. Detailed discussions about the wind field, continental outflow, vertical aerosol structure and possible reasons favouring the extreme aerosol loading in June 2008 are discussed by Prijith *et al.* (2013) and Kaskaoutis *et al.* (2014). Solomon *et al.* (2015) also reported an increase in dust activity over AS which caused a positive response of Indian monsoon precipitations on a weekly time scale.

The seasonal variation of AOD along with their standard

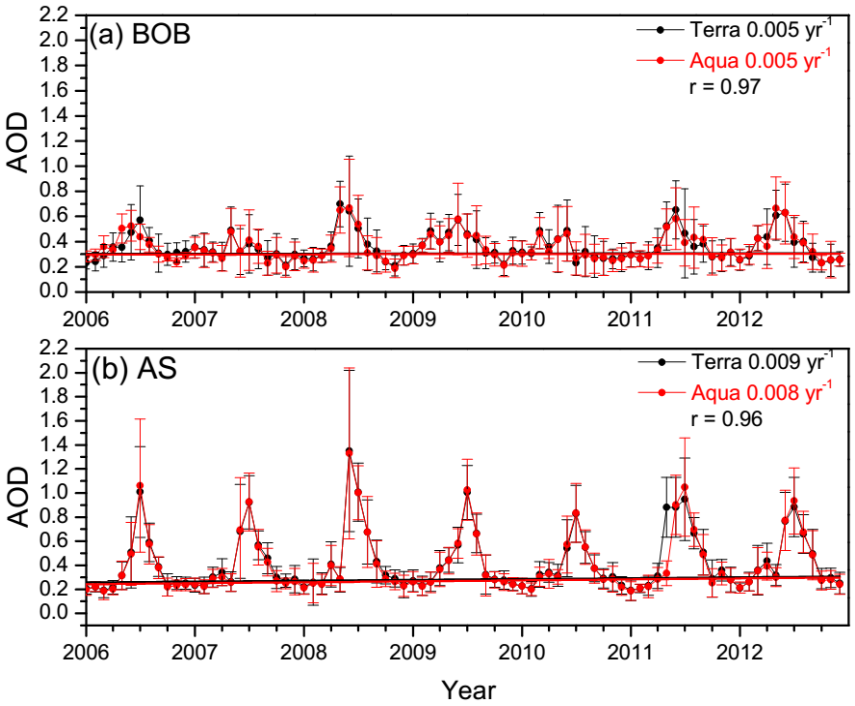

Fig. 2. Monthly mean time series of AOD during 2006–2012 over (a) BoB and (b) AS from MODIS on-board Terra and Aqua. The error bars represent the standard deviation for monthly mean. Trends of aerosol loading and the correlation coefficient (r) between MODIS Terra and Aqua is also given.

Table 1. Annual mean of AOD (550 nm) over BoB and AS.

Years	Annual Mean AOD (550 nm) with std deviation over BoB		Annual Mean AOD (550 nm) with std deviation over AS	
	Terra	Auqa	Terra	Auqa
2006	0.35 ± 0.12	0.35 ± 0.06	0.37 ± 0.12	0.36 ± 0.13
2007	0.33 ± 0.07	0.32 ± 0.08	0.40 ± 0.22	0.39 ± 0.22
2008	0.37 ± 0.16	0.36 ± 0.16	0.48 ± 0.36	0.47 ± 0.36
2009	0.39 ± 0.10	0.38 ± 0.10	0.41 ± 0.23	0.41 ± 0.24
2010	0.33 ± 0.09	0.33 ± 0.08	0.38 ± 0.18	0.37 ± 0.19
2011	0.37 ± 0.14	0.37 ± 0.14	0.48 ± 0.29	0.44 ± 0.29
2012	0.37 ± 0.14	0.38 ± 0.14	0.44 ± 0.22	0.43 ± 0.24

deviation is summarised in Table 3. It reflects that BoB has highest aerosol loading during the PrM season with highest associated standard deviation (0.44 ± 0.10) followed by the monsoon season (0.41 ± 0.09). The minimum average AOD is observed in the winter season with value 0.26 ± 0.09 followed by the PoM season with value 0.27 ± 0.03. AS experiences maximum aerosol loading in the monsoon season with the highest standard deviation (0.77 ± 0.22) followed by the PrM season (0.34 ± 0.14). However, AOD values are quite low in the PoM (0.33 ± 0.08) and winter (0.24 ± 0.03) seasons. Satheesh *et al.* (2006) also reported that average AOD values are 0.47 ± 0.14 and 0.29 ± 0.29 during the summer-monsoon (April/May–September) and winter-monsoon (November–March) season over AS which are somewhat similar to the present study. The results observed in the present study are quite comparable with Dey and Di Girolamo (2010) with a little different value which may be due to different meteorological parameters.

Climatology of Aerosol Vertical Distribution

Fig. 4 shows monthly mean variation of aerosol vertical profiles (backscatter at 532 nm) over (a) BoB and (b) AS during 2006–2012. The aerosol backscatter is a measure of aerosol loading. The maximum aerosol loading in the lower part of troposphere (boundary layer) is observed in May–August for both regions. AS experienced however, higher aerosol backscatter i.e., higher aerosol loading as compared to BoB, which is also corroborated with AOD variation over both the regions (Figs. 2 and 3). It shows the presence of elevated aerosol layers (up to 2–4 km) during May-August for almost every year of observation over both the regions. This could be attributed to the persistent long-range transportation of aerosols at higher altitude (1–3 km) during this period. However, again AS shows more pronounced vertically elevated aerosol during May–July than that over BoB. Prijith *et al.* (2013) have recently reported the highest values of aerosol extinction during June–August in 1–4 km

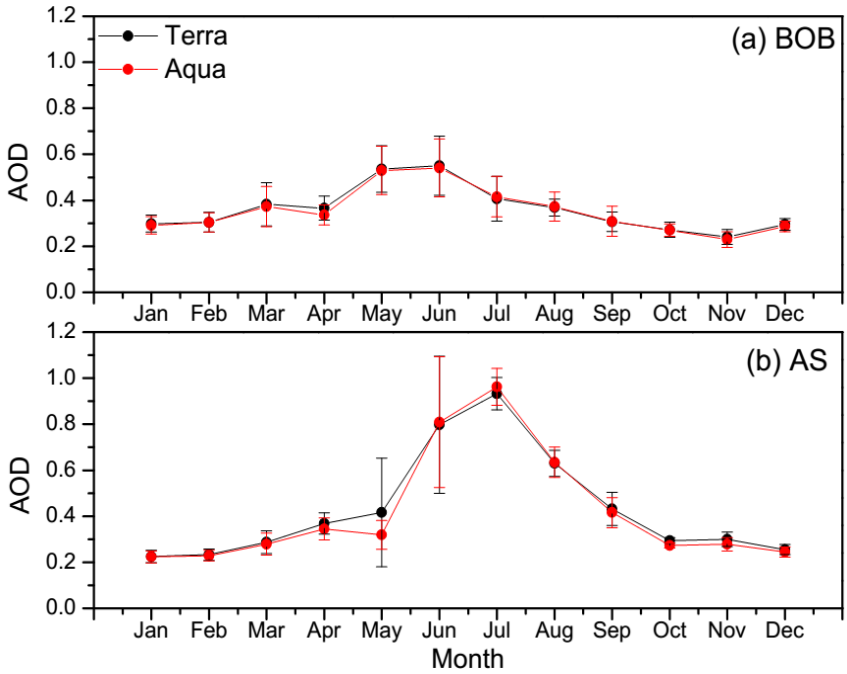

Fig. 3. Monthly mean variation of AOD during 2006–2012 over (a) BoB (b) AS. The error bars represent standard deviation.

Table 2. Monthly mean of AOD (550 nm) over BoB and AS during study period.

Months	Monthly Mean AOD (550 nm) with std deviation over BoB		Monthly Mean AOD (550 nm) with std deviation over AS	
	Terra	Auqa	Terra	Auqa
Jan	0.29 ± 0.04	0.28 ± 0.04	0.22 ± 0. 03	0.22 ± 0.03
Feb	0.30 ± 0.04	0.30 ± 0.04	0.23 ± 0.02	0.23 ± 0.02
Mar	0.37 ± 0.09	0.36 ± 0.09	0.27 ± 0.06	0.26 ± 0.06
Apr	0.36 ± 0.05	0.34 ± 0.04	0.35 ± 0.07	0.32 ± 0.07
May	0.51 ± 0.10	0.50 ± 0.12	0.40 ± 0.22	0.32 ± 0.06
Jun	0.54 ± 0.13	0.54 ± 0.13	0.76 ± 0.29	0.76 ± 0.28
Jul	0.43 ± 0.10	0.42 ± 0.09	0.94 ± 0.07	0.98 ± 0.08
Aug	0.37 ± 0.04	0.37 ± 0.06	0.62 ± 0.05	0.63 ± 0.06
Sep	0.31 ± 0.04	0.31 ± 0.07	0.43 ± 0.07	0.41 ± 0.06
Oct	0.28 ± 0.03	0.27 ± 0.03	0.29 ± 0.02	0.27 ± 0.02
Nov	0.25 ± 0.03	0.23 ± 0.03	0.29 ± 0.03	0.27 ± 0.03
Dec	0.30 ± 0.03	0.29 ± 0.02	0.25 ± 0.02	0.24 ± 0.02

Table 3. Seasonal mean variation of AOD (550 nm) over BoB and AS.

Season	Mean AOD (550 nm) over BoB	Mean AOD (550 nm) over AS
Per-monsoon	0.44 ± 0.10	0.34 ± 0.14
Monsoon	0.41 ± 0.09	0.77 ± 0.22
Post-monsoon	0.27 ± 0.03	0.33 ± 0.08
Winter	0.26 ± 0.09	0.24 ± 0.03

altitude range over AS (12–25°N; 57.5–72.5°E). These aerosols were characterized as transported non-spherical mineral dust, mainly coming from the Arabian desert region (Prijith *et al.*, 2013). Mishra *et al.* (2013) showed that these highly non-spherical dust plumes confined in 1–4 km altitude over AS could reach as far as Thiruvananthapuram (8.5°N, 77°E), a southernmost city in south India. A similar type of results are also observed over BoB under Integrated Campaign for Aerosols, Gases and Radiation Budget (ICARB) during March–May, 2006 using simultaneous lidar and in-situ measurements on-board an aircraft (Moorthy *et al.*, 2010). They reported the presence of elevated aerosol layers of enhanced extinction at altitudes of 1 to 3 km over BoB, which were associated with advection from west Asia and western India. The enhanced aerosol extinction at these altitude levels could be understood as Indian continental

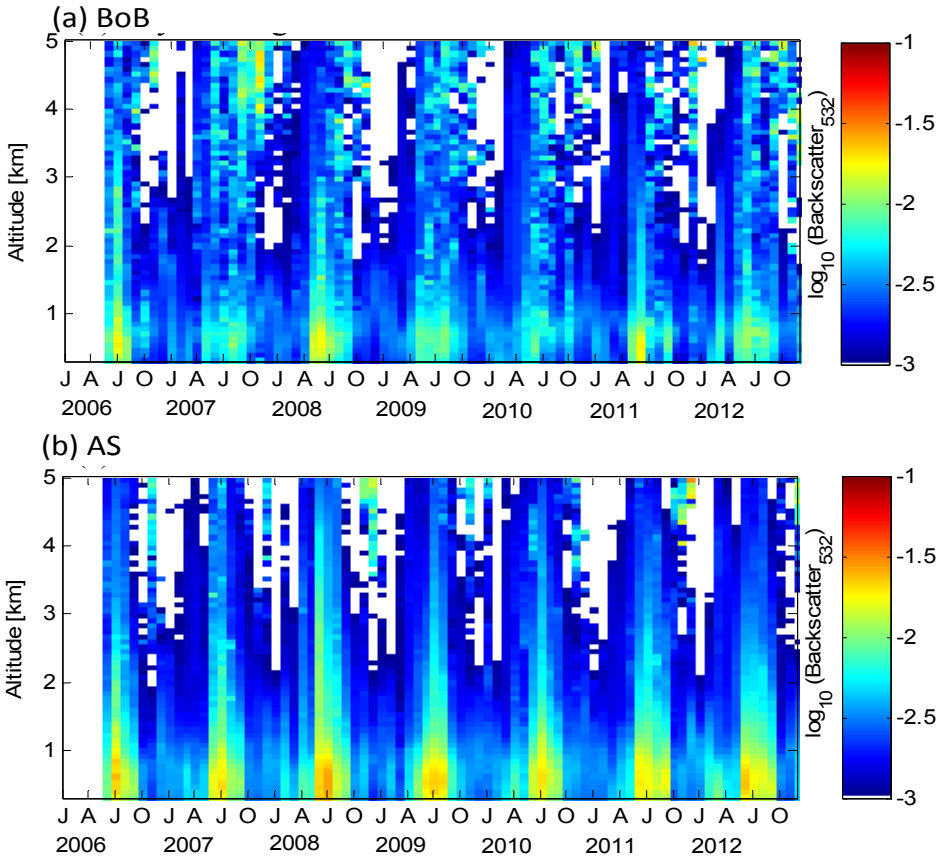

Fig. 4. Monthly mean variation of aerosol vertical profiles (backscatter at 532 nm) during 2006–2012 over (a) BoB and (b) AS from CALIOP night-time observations. The aerosol backscatter coefficients are shown in logarithmic scale.

outflow into BoB during the PrM and early monsoon seasons (Campbell *et al.*, 2013). Fig. 4 also shows the presence of elevated aerosol layers at higher altitudes (> 4 km) during October–November over both regions, but more pronounced over BoB. These elevated aerosol layers, especially over BoB could be the result of the long-range transportation of agricultural biomass burning aerosols from Indo Gangetic Basin (IGB) region (Badarinath *et al.*, 2009; Mishra *et al.*, 2012b). It has been shown that the elevated layers of agricultural crop residue burning aerosols, originating from north-western part of IGB (Mishra *et al.*, 2012b; Tiwari and Singh, 2013) could be transported to a long distance as far as AS and eastern part of India (Badarinath *et al.*, 2009) during October–November. Over both the regions, December–February was characterized as relatively lower aerosol backscatter and confined aerosol layers near the sea surface, which was also consistent with AOD observation from MODIS. This result could be rationalised by relatively stable meteorological conditions during the winter season (Kar *et al.*, 2010; Mishra et al., 2012a and references therein), which could inhibit the long-range transportation of polluted air-masses from land to oceanic regions.

In order to study the inter-annual periodicity and relative strength of transported aerosol loading over both the regions, we have plotted monthly mean time series of averaged aerosol backscatter between 1.0 to 3.0 km altitudes for BoB and AS during 2006–2012 (Fig. 5). In general, both the regions showed periodic nature of transported aerosol backscatter variability with a peak during May–August in every year. However, aerosol backscatter coefficients are significantly higher over AS than that over BoB during this period for most of the years. The peaks in aerosol backscatter have almost one month lag for both of the regions: i.e., July over AS and June over BoB. These observations could be easily seen in Fig. 6, where 7 years monthly averaged (2006–2012) aerosol backscatter coefficient were found maximal in July ($5.26 \pm 0.55 \times 10^{-3}$ km^{-1} sr^{-1}) over AS and in June ($3.89 \pm 0.52 \times 10^{-3}$ km^{-1} sr^{-1}) over BoB. Fig. 6 shows that both the regions experiences almost similar aerosol loading during January–April, but AS experiences relatively more aerosol loading in June–August and BoB experienced more in September–December. These lidar observed results (Fig. 6) also corroborated with radiometric measurements from MODIS in terms of aerosol loading over both the regions (Fig. 3).

Seasonal Variation of Aerosol Types

In order to classify the seasonal aerosol types over the study regions, a scatter plot between aerosol index (AI) retrieved from OMI, aerosol fine mode fraction (FMF), and Angstrom exponent (AE) between a pair of wavelength 550 and 865 nm retrieved from MODIS is plotted and shown in Fig. 7. FMF is a ratio of fine aerosol optical depth and total optical depth, which qualitatively tells

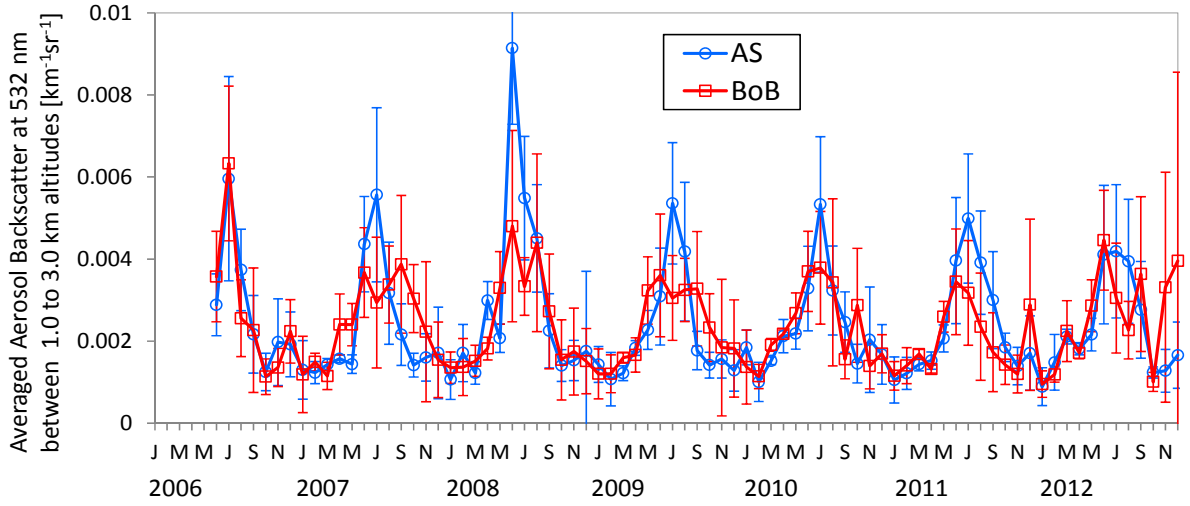

Fig. 5. Monthly mean time series of averaged aerosol backscatter [km^{-1} sr^{-1}] at 532 nm between 1.0 to 3.0 km altitudes for BoB and AS during 2006–2012. The error bars represent standard deviation for monthly mean values.

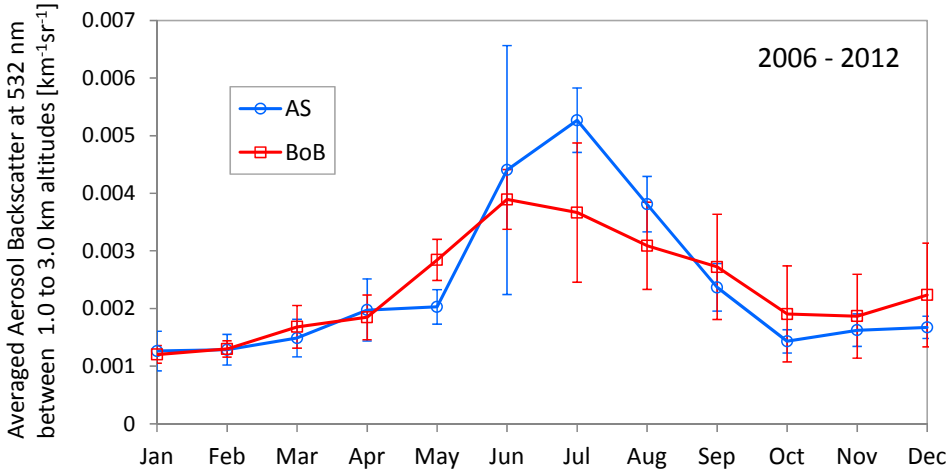

Fig. 6. Monthly mean time series of averaged aerosol backscatter [km^{-1} sr^{-1}] at 532 nm between 1.0 to 3.0 km altitudes for BoB and AS during 2006–2012. The error bars represent standard deviation for monthly mean values.

about the particle size distribution similar to AE. AI is a qualitatively good indicator of absorbing aerosol and their altitudes in troposphere (Herman *et al.*, 1997; Torres *et al.*, 2013). The higher values of AI (> 1) represent absorbing type of aerosols (like dust and biomass burning aerosols) residing at relatively higher altitude. However, lower positive values or negative values suggest the existence of non-absorbing aerosol particles below certain altitude leve (Prospero *et al.*, 2002). Fig. 7 reflects an abundance of aerosol loading with a large seasonal heterogeneity in AI and FMF values over the both the regions due to various emission sources. Fig. 7(a) shows that the PrM and monsoon season are characterized by a wide range of FMF with the higher values of AI over BoB, which suggest a mixture of absorbing aerosol loading (dust and biomass burning). However, on few days AI values reach > 2 which may be due to elevated dust aerosols, which were coming over the region due to the long range transportation. Sreekanth *et al.* (2013) also reported a higher value of AI associated with a lower value of small mode fraction aerosol particles over north BoB during the PrM season. In the winter season during most of the days (99%) the observed values of FMF > 0.5 along with the higher values of AI (AI > 1 during 91% days) suggesting a dominance of mixed urban-industrial pollution and smoke/biomass burning type absorbing aerosols. Earlier studies also suggested an enhancement in fine mode aerosol loading during the PoM and winter season over BoB due to biomass burning and combustion sources (Nair *et al.*, 2010; Kaskaoutis *et al.*, 2011). Fig. 7(c) shows that high AI values are associated with relatively smaller values of FMF (i.e., FMF < 0.5) over AS during the monsoon season, suggesting the dominance of dust aerosol particles which were mainly coming from the Middle East region at higher altitude which can be also confirmed from air mass back trajectories analysis discussed in next section. Recently Kaskaoutis *et al.* (2014) also reported a heavy dust over AS during the monsoon season coming from Sistan region due to long range transportation. Prijith *et al.* (2013) also reported relatively

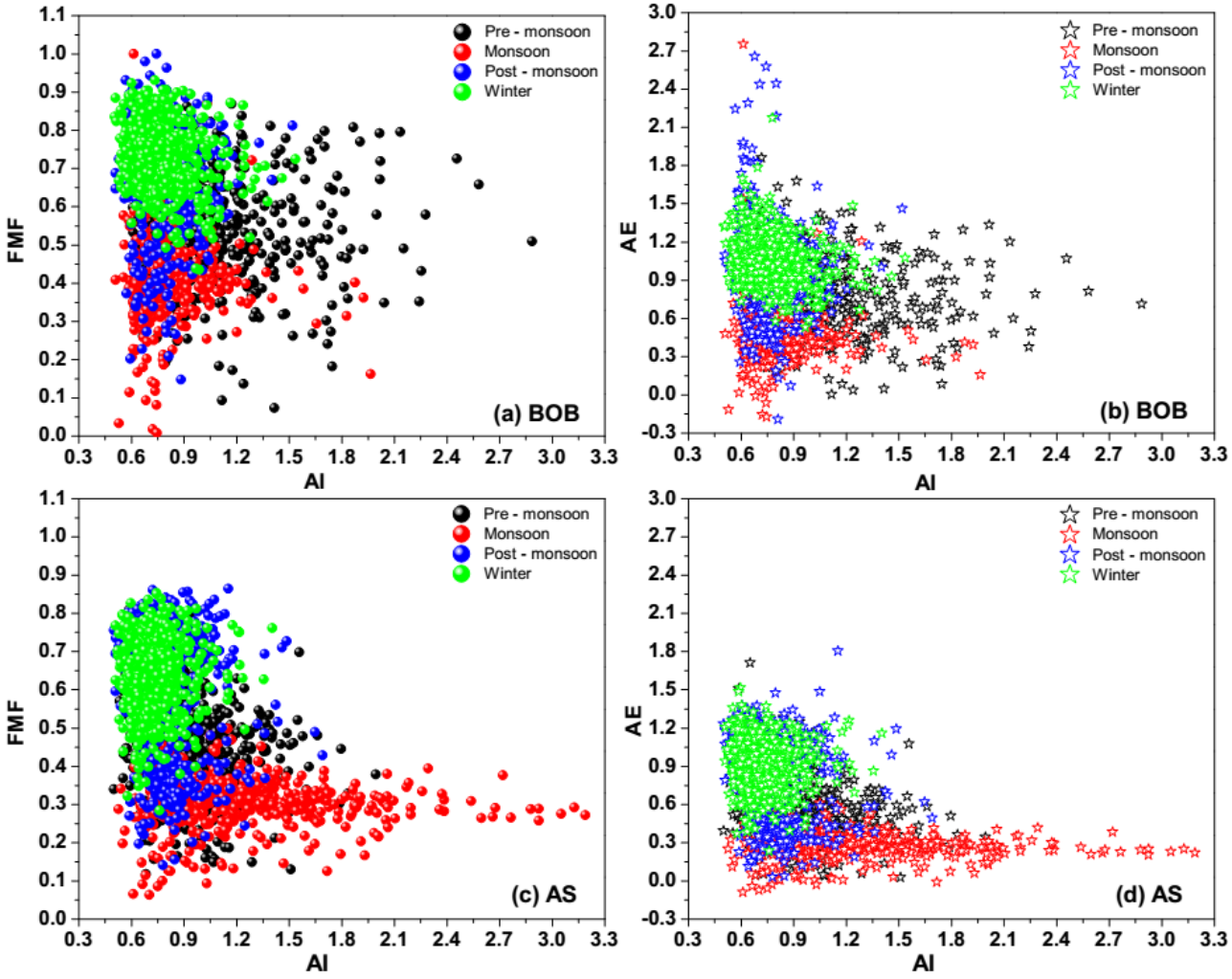

Fig. 7. Seasonal scatter plot between OMI-derived Aerosol Index (AI) vs. MODIS-derived Fine Mode Fraction (FMF) and Aerosol Index (AI) vs. MODIS-derived Aerosol Angstrom ($AE_{550–865\ nm}$) over BoB and AS during 2006–2012. Each data point present daily mean values over AS/BoB region.

high aerosol loading in June over AS. Babu *et al.* (2008) and Moorthy *et al.* (2009) also suggested a significant amount of aerosol loading over the oceanic-atmospheric boundary layer up to 2 to 4 km. However, during the PoM and winter season, the relatively higher values of FMF associated with relatively lower values of AI are indicating the dominance of absorbing smoke (mainly from biomass burning and fossil fuel) coming from the near-by coastal regions or via long range transportation. A wide range of FMF values observed along with higher values of AI were indicating a mixture of different types of aerosol loading over AS during the PrM season with the dominant contribution from dust particles. Several studies also reported heterogeneity in aerosol types loading over AS during the PrM season (Moorthy *et al.*, 2005; Satheesh *et al.*, 2006; Kedia and Ramchandran, 2008; Kalapureddy *et al.*, 2009; Kaskaoutis *et al.*, 2010 and reference therein). Similar to FMF vs. AI (Figs. 7(a) and 7(c)) plots, Figs. 7(b) and 7(d) show scatter plot between AE and AI over BoB and AS, respectively. Higher values of AE show dominance of fine mode particles, whereas lower values depict dominance of coarse mode particles. The similar explanations could be drawn for AE vs. AI as discussed for FMF vs. AI over both the regions.

Examination of Aerosol Transportation Using HYSPLIT

Soil dust, biomass burning/biofuel, biogenic sulphur particles and other anthropogenic aerosol particles from the adjoining landmass are transported by the synoptic scale wind pattern and superimposed over sea salt aerosol particles. These anthropogenic aerosol masking could greatly influence the solar radiation budget over the oceanic regions. Seven days air mass back trajectories were computed using NOAA HYSPLIT back trajectories model at three different altitude levels (viz. 500 m, 1500 m, and 2500 m). The seasonal mean (2006–2012) back trajectories results for BoB and AS are presented in Figs. 8 and 9, respectively. Fig. 8(a) shows that at higher altitude level air masses are coming from longer distance (i.e., from the Middle East and the Thar Desert) carrying a lot of dust particles during the PrM season over BoB, which are also shown by CALIOP analysis (Figs. 4(a) and 5). It may be due to heat convection which uplift air masses and in aggregation with strong surface wind form a

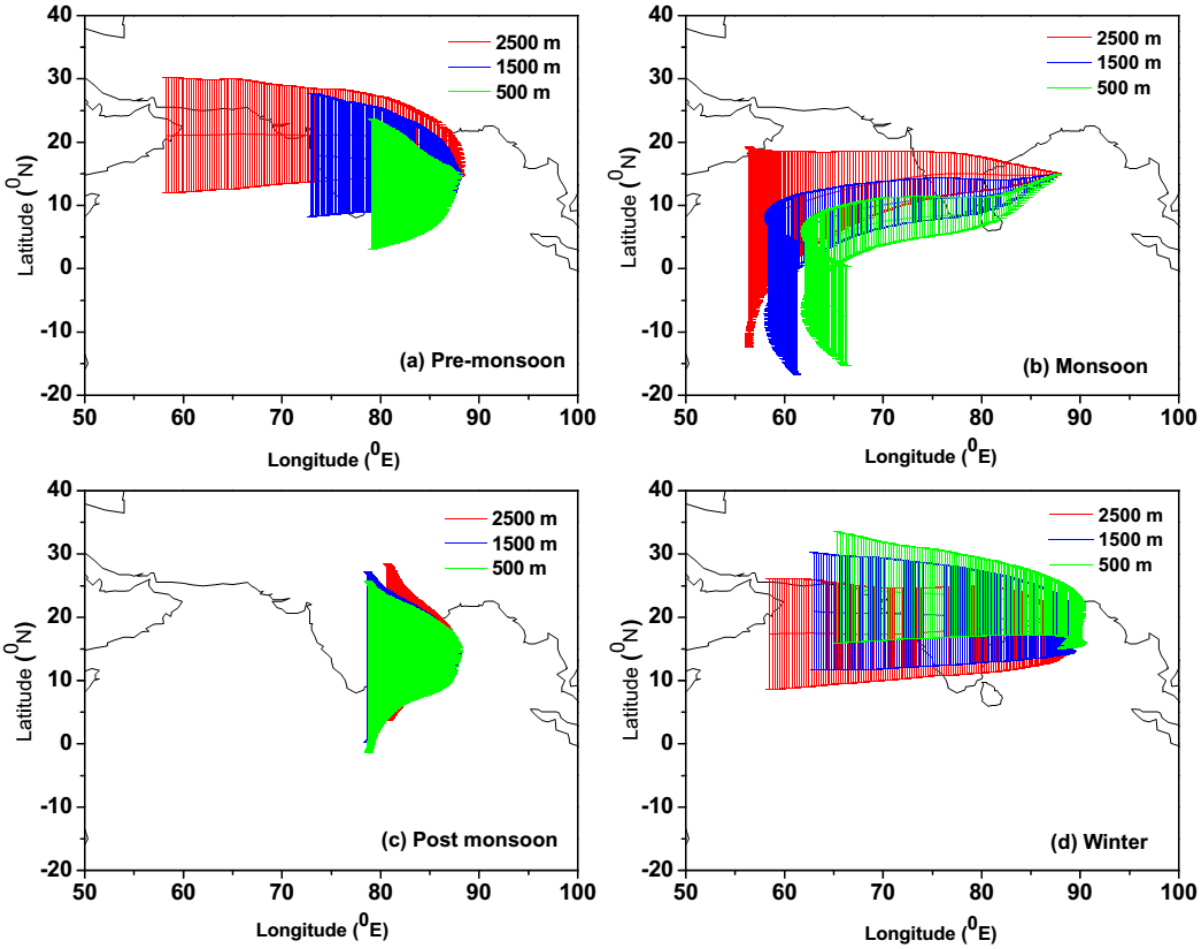

Fig. 8. Averaged seasonal (2006–2012) air mass back trajectories over BoB at three different altitude level viz. 500 m, 1000 m and 2500 m. The vertical lines show standard deviation, representing latitudinal air-mass spreading.

dust storm containing the abundance of coarse mode aerosol particles (Tiwari *et al.*, 2015). In the monsoon season, air masses are coming from the Indian ocean passes through AS which itself experience a high aerosol loading during this season (Prijith *et al.*, 2013; Kaskaoutis *et al.*, 2014 and reference therein). In the post-monsoon season, aerosols coming over BoB from the local land emission sources have dominance of fine mode particles, which are also confirmed from Fig. 8(c). In the winter season, air masses at higher level altitude are mainly coming from AS through north-India, while at low altitude level air masses were coming from north-India with a lot of fine mode aerosol particles. Krishnamurthi *et al.* (2009) reported that the aerosols from the AS significantly affect the aerosol loading over BoB through long-range transportation. Fig. 9 shows that during the pre-monsoon and winter season, aerosols are coming from the Middle East at all the altitude levels over AS. In the monsoon season, air masses are coming from the Middle East at higher altitudes carrying a lot of dust over AS. However, AS is influenced by pristine oceanic wind coming from the Indian Ocean at lower altitude levels. In the PoM season, aerosols are mainly coming from north-west Indian continent containing dominance of fine mode aerosol particles which is also confirmed from Fig. 9(c).

CONCLUSION

Aerosol climatology and seasonal variability along with vertical distribution of various types of aerosol loading is studied over the AS and BoB using long-term (2006–2012) observations from space-borne radiometers and lidar. AOD observations over both the study regions show strong seasonal and interannual variability. The maximum aerosol loading is observed in the monsoon season followed by the PrM season over AS. However, BoB experiences an opposite pattern in aerosol loading i.e., maximum in PrM followed by the monsoon season. Relatively lower aerosol loading is observed over both the regions during PoM and winter season. Maximum AOD is found in July followed by June month over AS. We find a one month lag between AS and BoB for maximum aerosol loading in all years of observations, which is explained using synoptic wind pattern and air-mass back trajectories analysis. The elevated aerosol layers (up to 2–4 km) are also found during May-August (PrM and M season) over both regions with more prominent over AS than BOB that could be rationalised by higher fraction of long range transported aerosols at higher altitude over AS. The elevated aerosol layers > 4 km are also observed during October–November (PoM) which is

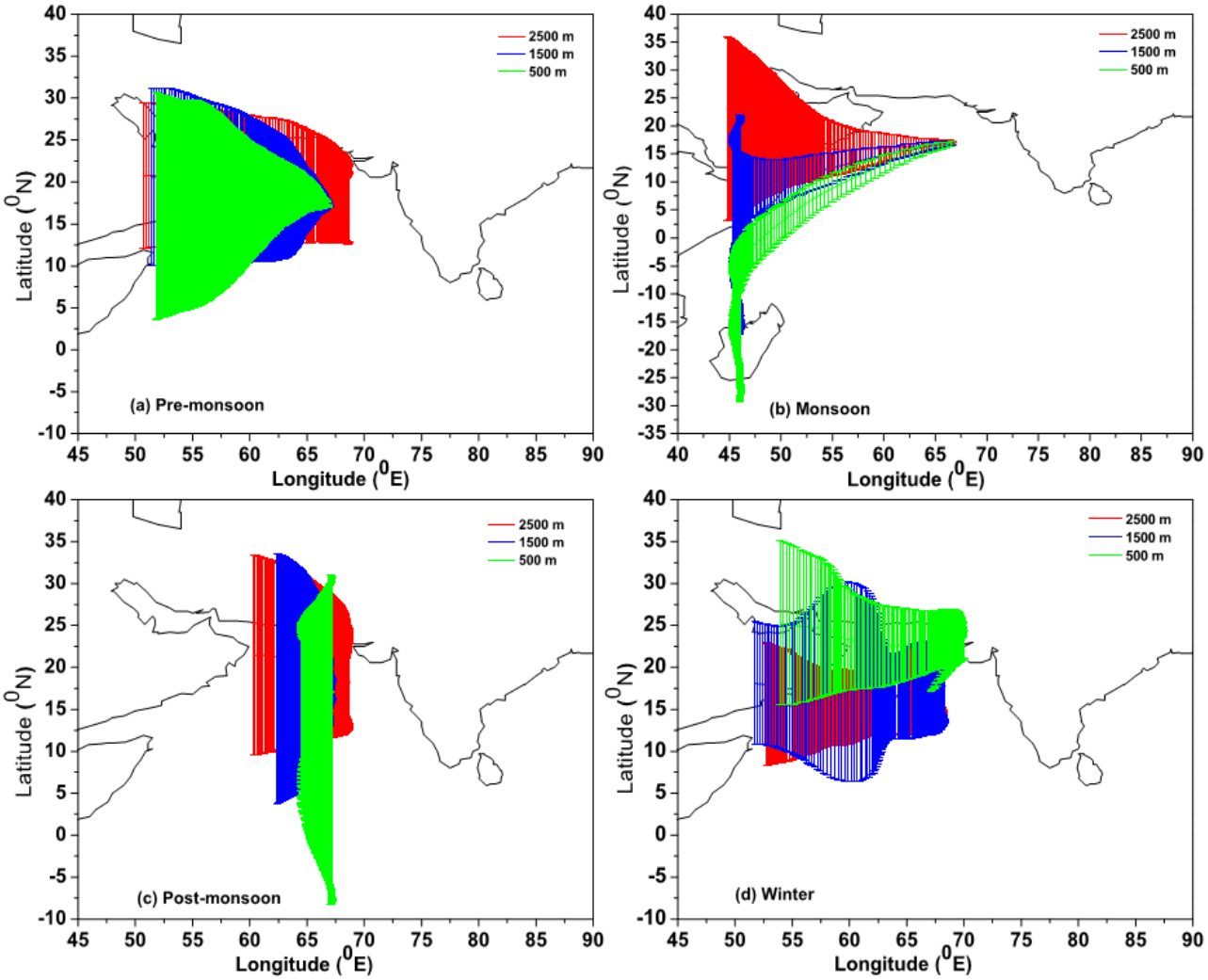

Fig. 9. Averaged seasonal (2006–2012) air mass back trajectories over AS at three different altitude level viz. 500 m, 1000 m and 2500 m. The vertical lines show standard deviation, representing latitudinal air-mass spreading.

more prominent over BoB than AS because of dominant long-range transportation of agricultural biomass burning aerosols from the IGB region. AI vs. FMF and AI vs. AE analyses show seasonal heterogeneity in aerosol behaviour over the both oceanic regions. This seasonal heterogeneity could be understood as the effect of long range/short range transportation from various emission sources on aerosol properties over the oceanic region. The present study also indicates the possible role of Indian summer monsoon in modulating the aerosol behaviour over AS and BoB, which needs further deep inspection with higher temporal/spatial resolution data.

ACKNOWLEDGEMENT

We are thankful to MODIS NASA group for providing aerosol data. We acknowledge the use of National Centre for Environmental Prediction (NCEP) for synoptic meteorological data and NOAA HYSPLIT model for back-trajectory analysis. One of the authors, Mr S. Tiwari is also thankful to CSIR, New Delhi for providing senior research fellowship. The work is partly supported by ISRO, Bangalore under ISRO-SSPS. We are grateful to the two anonymous reviewers for their constructive comments and suggestions to improve the quality of manuscript.

REFERENCES

Babu, S.S., Nair, V.S. and Moorthy K.K. (2008). Seasonal changes in aerosol characteristics over Arabian Sea and their consequence on aerosol short-wave radiative forcing: Results from ARMEX field campaign. *J. Atmos. Sol. Terr. Phys.* 70: 820–834.

Badarinath, K.V.S., Kharol, S.K., Sharma, A.R. and Krishna Prasad, V. (2009b). Analysis of aerosol and carbon monoxide characteristics over Arabian Sea during crop residue burning period in the Indo-Gangetic Plains using multi-satellite remote sensing datasets. *J. Atmos. Sol. Terr. Phys.* 71: 1267–1276.

Boucher, O., Randall, D., Artaxo, P., Bretherton, C., Feingold, G., Forster, P., Kerminen, V.M., Kondo, Y., Liao, H., Lohmann, U., Rasch, P., Satheesh, S.K., Sherwood, S.,

Stevens, B. and Zhang, X.Y. (2013). Clouds and Aerosols. In *Climate Change 2013: The Physical Science Basis*. Contribution of Working Group II of the Fifth Assessment Report of the Intergovernmental Panel on Climate Change, Stocker, T.F., Qin, D., Plattner, G.K., Tignor, M., Allen, S.K., Boschung, J., Nauels, A., Xia, Y., Bexand, V. and Midgley, P.M. (Eds.), Cambridge University Press, Cambridge, United Kingdom and New York, NY, USA.

Campbell, J.R., Reid, J.S., Westphal, D.L., Zhang, J., Tackett, J.L., Chew, B.N., Welton, E.J., Shimizu, A., Sugimoto, N., Aoki, K. and Winker, D.M. (2013). Characterizing the vertical profile of aerosol particle extinction and linear depolarization over Southeast Asia and the Maritime Continent: The 2007–2009 view from CALIOP. *Atmos. Res.* 12: 520–543.

Dey, S., Sarkar, S. and Singh, R.P. (2004). Comparison of aerosol radiative forcing over the Arabian Sea and the Bay of Bengal. *Adv. Space Res.* 33: 1104–1108.

Dey, S. and Di Girolamo, L. (2010). A climatology of aerosol optical and microphysical properties over the Indian subcontinent from 9 years (2000–2008) of Multiangle Imaging Spectroradiometer (MISR) data. *J. Geophys. Res.* 115: D15204.

Draxler, R.R. and Rolph, G.D. (2003). *HYSPLIT (Hybrid Single-Particle Lagrangian Integrated Trajectory) Model*. NOAA Air Resources Laboratory, Silver Spring, MD.

Herman, J., Bhartia, P., Torres, O., Hsu, C., Seftor, C. and Celarier, E. (1997). Global distribution of UV-absorbing aerosols from Nimbus 7/TOMS data. *J. Geophys. Res.* 102: 16911–16922.

Kar, J., Deeter, M.N., Fishman, J., Liu, Z., Omar, A., Creilson, J.K., Trepte, C.R., Vaughan, M.A. and Winker, D.M. (2010). Wintertime pollution over the Eastern Indo-Gangetic Plains as observed from MOPITT, CALIPSO and tropospheric ozone residual data. *Atmos. Chem. Phys.* 10: 12273–12283.

Kaskaoutis, D.G., Kalapureddy, M.C.R., Krishnamoorthy, K., Devara, P.C.S., Nastos, P.T., Kosmopoulos, P.G. and Kambezidis, H.D. (2010). Heterogeneity in pre-monsoon aerosol types over the Arabian Sea deduced from ship-borne measurements of spectral AODs. *Atmos. Chem. Phys.* 10: 4893–4908.

Kaskaoutis, D.G., Kumar Kharol, S., Sinha, P.R., Singh, R.P., Kambezidis, H.D., Rani Sharma, A. and Badarinath, K.V.S (2011). Extremely large anthropogenic aerosol component over the Bay of Bengal during winter season. *Atmos. Chem. Phys.* 11: 7097–7117.

Kaskaoutis, D.G., Rashki, A. Houssos, E.E., Goto, D. and Nastos, P.D. (2014). Extremely high aerosol loading over Arabian Sea during June 2008: The specific role of the atmospheric dynamics and Sistan dust storms. *Atmos. Environ.* 94: 374–384.

Kaufman, Y.J., Tanré, D., Remer, L.A., Vermote, E.F., Chu, A. and Holben, B.N. (1997). Operational remote sensing of tropospheric aerosol over land from EOS moderate resolution imaging spectroradiometer. *J. Geophys. Res.* 102: 17051–17068.

Kaufman, Y.J. and Tanrè, D. (1998). Algorithm for Remote Sensing of Tropospheric Aerosol from MODIS. Algorithm Theoretical Basis Documents 85: ATBD-MOD-02.

Kedia, S. and Ramachandran, S. (2008). Features of aerosol optical depths over the Bay of Bengal and the Arabian Sea during premonsoon season: Variabilities and anthropogenic influence. *J. Geophys. Res.* 113: D11201.

Krishnamurti, T.N., Chakraborty, A., Martin, A., Lau, W.K., Kim, K.M., Sud, Y. and Walker, G. (2009). Impact of Arabian Sea pollution on the Bay of Bengal winter monsoon rain. *J. Geophys. Res.* 114: D06213.

Kumar, A., Sarin, M.M. and Srinivas B. (2010). Aerosol iron solubility over Bay of Bengal: Role of anthropogenic sources and chemical processing. *Mar. Chem*. 121: 167–175.

Labonne, M., Bréon, F.M. and Chevallier, F. (2007), Injection height of biomass burning aerosols as seen from a spaceborne lidar. *Geophys. Res. Lett.* 34: L11806.

Levelt, P.F., van den Oord, G.H.J., Dobber, M.R., Malkki, A., Huib, V., Johan de, V., Stammes, P., Lundell, J.O.V. and Saari, H. (2006). The ozone monitoring instrument. *IEEE Trans. Geosci. Remote Sens.* 44: 1093–1101.

Mishra, A.K., Klingmueller, K., Fredj, E., Lelieveld, J., Rudich, Y. and Koren, I. (2014). Radiative signature of absorbing aerosol over the eastern Mediterranean basin. *Atmos. Chem. Phys.* 14: 7213–7231.

Mishra, A.K. and Shibata, T. (2012a). Climatological aspects of seasonal variation of aerosol vertical distribution over central Indo-Gangetic belt (IGB) inferred by the space-borne lidar CALIOP. *Atmos. Environ.* 46: 365–375.

Mishra, A.K. and Shibata, T. (2012b). Synergistic analyses of optical and microphysical properties of agricultural crop residue burning aerosols over the Indo-Gangetic Basin (IGB). *Atmos. Environ.* 57: 205–218.

Mishra, M.K., Rajeev, K., Thampi, B.V. and Nair, A.K.M. (2013). Annual variations of the altitude distribution of aerosols and effect of long-range transport over the southwest Indian Peninsula. *Atmos. Environ.* 81: 51–59.

Moorthy, K.K., Niranjan, K., Narasimhamurthy, B., Agashe, V.V. and Murthy, B.V.K. (1999). Aerosol Climatology over India, 1. ISRO GBP MWR Network and Database, Scientific Report, ISRO GBP, SR 03 99. Indian Space Research Organisation, India.

Moorthy, K.K. and Satheesh, S.K. (2000). Characteristics of aerosols over a remote island, Minicoy in the Arabian Sea: Optical properties and retrieved size characteristics. *Q. J. R. Meteorolog. Soc.* 126: 81–109.

Moorthy, K.K., Babu, S.S. and Satheesh, S.K. (2005). Aerosol characteristics and radiative impacts over the Arabian Sea during the inter-monsoon season: Results from ARMEX field campaign. *J. Atmos. Sci.* 62: 192–206.

Moorthy, K.K., Nair, V.S., Babu, S.S. and Satheesh, S.K. (2009). Spatial and vertical heterogeneities in aerosol properties over oceanic regions around India: Implications for radiative forcing. *Q. J. R. Meteorolog. Soc.* 135: 2131–2145.

Nair, S.K., Parameswaran, K. and Rajeev, K. (2005). Seven year satellite observations of the mean structures and variabilities in the regional aerosol distribution over the oceanic areas around the Indian subcontinent. *Ann. Geophys.* 23: 1–20.

Nair, V.S., Satheesh, S.K., Moorthy, K.K., Babu, S.S., Nair, P.R. and George, S.K. (2010). Surprising observation of large anthropogenic aerosol fraction over the "near-pristine" southern Bay of Bengal: Climate implications. *J. Geophys. Res.* 115: D21201.

Nair, V.S., Moorthy, K.K. and Babu, S.S. (2013). Influence of continental outflow and ocean biogeochemistry on the distribution of fine and ultrafine particles in the marine atmospheric boundary layer over Arabian Sea and Bay of Bengal. *J. Geophys. Res.* 118: 7321–7331.

Prijith, S.S., Rajeev, K., Thampi, B.V., Nair, S.K. and Mohan, M. (2013). Multi-year observations of the spatial and vertical distribution of aerosols and the genesis of abnormal variations in aerosol loading over the Arabian Sea during Asian summer monsoon season. *J. Atmos. Sol. Terr. Phys.* 105–106: 142151.

Prospero, J.M., Ginoux, P., Torres, O., Nicholson, S.E. and Gill, T.E. (2002). Environmental characterization of global sources of atmospheric soil dust identified with the Nimbus 7 Total Ozone Mapping Spectrometer (TOMS) absorbing aerosol product. *Rev. Geophys.* 40: 1002.

Ramanathan, V., Crutzen, P.J., Andreae, M.O., Coakley, J., Dickerson, R., Heintzenberg, J., Heymsfield, A., Kiehl, J.T., Kley, D., Krishnamurti, T.N., Kuettner, J., Lelieveld, J., Liu, S.C., Mitra, A.P., Prospero, J., Sadourny, R., Tuck, A.F. and Valero, F.P.J. (1995). *Indian Ocean Experiment (INDOEX) White Paper*, C4, Scripps Inst. of Oceanography, UCSD, La Jolla, Calif.,

Ramanathan, V., Crutzen, P.J., Lelieveld, J., Mitra, A.P., Althausen, D., Anderson, J., Andreae, M.O., Cantrell, W., Cass, G.R., Chung, C.E., Clarke, A.D., Coakley, J.A., Collins, W.D., Conant, W.C., Dulac, F., Heintzenberg, J., Heymsfield, A.J., Holben, B., Howell, S., Hudson, J., Jayaraman, A., Kiehl, J.T., Krishnamurti, T.N., Lubin, D., McFarquhar, G., Novakov, T., Ogren, J.A., Podgorny, I.A., Prather, K., Priestley, K., Prospero, J.M., Quinn, P.K., Rajeev, K., Rasch, P., Rupert, S., Sadourny, R., Satheesh, S.K., Shaw, G.E., Sheridan, P. and Valero, F.P.J. (2001). Indian Ocean Experiment: An integrated analysis of the climate forcing and effects of the great Indo-Asian haze. *J. Geophys. Res.* 106: 28371–28398.

Remer, L.A., Kaufman, Y.J., Tanré, D., Mattoo, S., Chu, D.A., Martins, J.V., Li, R.R., Ichoku, C., Levy, R.C., Kleidman, R.G., Eck, T.F., Vermote, E. and Holben, B.N. (2005). The MODIS aerosol algorithm, products, and validation. *J. Atmos. Sci.* 62: 947–973.

Remer, L.A., Kleidman, R.G., Levy, R.C., Kaufman, Y.J., Tanre, D., Mattoo, S., Martins, J.V., Ichoku, C., Koren, I., Yu, H. and Holben, B.N. (2008). Global aerosol climatology from the MODIS satellite sensors. *J. Geophys. Res.* 113: D14S07.

Satheesh, S.K., Moorthy, K.K. and Das, I. (2001). Aerosol spectral optical depths over the Bay of Bengal, Arabian Sea and Indian Ocean. *Curr. Sci.* 81: 1617–1625.

Satheesh, S.K., Moorthy, K.K., Kaufman, Y.J. and Takemura, T. (2006). Aerosol optical depth, physical properties and radiative forcing over the Arabian Sea. *Meteorol. Atmos. Phys.* 91: 45–62.

Satheesh, S.K., Vinoj, V. and Moorthy, K.K. (2010). Assessment of aerosol radiative impact over oceanic regions adjacent to Indian subcontinent using multisatellite analysis. *Adv. Meteorol.* 2: 139186.

Smirnov, A., Villevalde, Y., O'Neill, N.T., Royer, A. and Tarussov, A. (1995). Aerosol optical depth over the oceans: Analysis in terms of synoptic air mass types. *J. Geophys. Res.* 100: 16639–16650.

Smirnov, A., Holben, B.N., Slutsker, I., Giles, D.M., McClain, C.R., Eck, T.F., Sakerin, S.M., Macke, A., Croot, P., Zibordi, G., Quinn, P.K., Sciare, J., Kinne, S., Harvey, M., Smyth, T.J., Piketh, S., Zielinski, T., Proshutinsky, A., Goes, J.I., Nelson, N.B., Larouche, P., Radionov, V.F., Goloub, P., Krishna Moorthy, K., Matarrese, R., Robertson, E.J. and Jourdin, F. (2009). Maritime aerosol network as a component of aerosol robotic network. *J. Geophys. Res.* 114: D06204.

Solomon, A., Feingold, G. and Shupe, M.D. (2015). The role of ice nuclei recycling in the maintenance of cloud ice in Arctic mixed-phase stratocumulus. *Atmos. Chem. Phys.* 15: 10631–10643.

Sreekanth, V. and Kulkarni, P. (2013). Spatio-temporal variations in columnar aerosol optical properties over Bay of Bengal: Signatures of elevated dust. *Atmos. Environ.* 69: 249–257.

Tindale, N.W. and Pease, P.P., (1999). Aerosols over the Arabian Sea: Atmospheric transport pathways and concentrations of dust and sea salt. *Deep Sea Res. Part II* 46: 1577–1595.

Tiwari, S. and Singh, A.K. (2013). Variability of aerosol parameters derived from ground and satellite measurements over Varanasi located in the Indo-Gangetic Basin. *Aerosol Air Qual. Res.* 13: 627–638.

Tiwari, S., Srivastava, A.K. and Singh, A.K. (2013). Heterogeneity in pre-monsoon aerosol characteristics over the Indo-Gangetic Basin. *Atmos. Environ.* 77: 738–747.

Tiwari, S., Srivastava, A.K., Singh, A.K. and Singh, S. (2015). Identification of aerosol types over Indo-Gangetic Basin: Implications to optical properties and associated radiative forcing. *Environ. Sci. Pollut. Res.* 22: 12246–12260.

Torres, O., Tanskanen, A., Veihelmann, B., Ahn, C., Braak, R., Bhartia, P.K., Veefkind, P. and Levelt, P. (2007). Aerosols and surface UV products from Ozone Monitoring Instrument observations: An overview. *J. Geophys. Res.* 112: D24S47.

Torres, O., Ahn, C. and Chen, Z. (2013). Improvements to the OMI near-UV aerosol algorithm using A-train CALIOP and AIRS observations. *Atmos. Meas. Tech.* 6: 3257–3270.

Vinoj, V., Babu, S.S., Satheesh, S.K., Moorthy, K.K. and Kaufman, Y.J. (2004). Radiative forcing by aerosols over the Bay of Bengal region derived from shipborne, island-based, and satellite (Moderate-Resolution Imaging Spectroradiometer) observations. *J. Geophys. Res.* 109: D05203.

Wild, M. (2009). Global dimming and brightening: A review. *J. Geophys. Res.* 114: D00D16.

Winker, D.M., Hunt, W.H. and McGill, M.J., (2007).

Initial performance assessment of CALIOP. *Geophys. Res. Lett.* 34: L19803.

Young, S.A. and Vaughan, M.A. (2008). The retrieval of profiles of particulate extinction from Cloud Aerosol Lidar Infrared Pathfinder Satellite Observations (CALIPSO) data: Algorithm description. *J. Atmos. Oceanic Technol.* 26: 1105–1119.

Received for review, June 27, 2015
Revised, December 11, 2015
Accepted, December 11, 2015